Unitary Design of Radar Waveform Diversity Sets

Michael D. Zoltowski, Tariq R. Qureshi, Robert Calderbank, and William Moran

***Abstract*— In this work, multiple radar waveforms are simultaneously transmitted, emitted from different "virtual" antennas. The goal is to process the returns in such a way that the overall ambiguity function is a sum of ambiguity functions better approximating the desired thumbtack shape. A 4×4 example involves two spatially separated antennas with each able to transmit and receive simultaneously on two different polarizations. The 4×4 unitary design dictates the scheduling of the waveforms over the four virtual antennas over four PRIs (Pulse Repetition Intervals), and how the matched filtering of the returns over four PRIs is combined in to achieve both perfect separation (of the superimposed returns) and perfect reconstruction. Perfect reconstruction means the sum of the time-autocorrelations associated with each of the four waveforms is a delta function. Conditions for both perfect separation and perfect reconstruction are developed, and a variety of waveform sets satisfying both are presented.**

I. Introduction

In active sensing systems, the objective is to design a communication system that allows one to learn the environment, which could be one or more moving targets in the case of a radar. In a radar system, the transmitted waveforms are reflected by the target and the reflected returns are then processed at the receiving end to determine the location(delay) and speed(doppler) of the target. Therefore, it is desired to transmit a waveform that provides good resolution in terms of the delay-doppler properties of the radar returns. This is characterized by the use of ambiguity functions, which measure the delay doppler correlation of the received waveforms with the actual transmitted waveform. The ambiguity function [1] of a waveform $s(t)$ is given by

$$\chi(\tau, \upsilon) = \int_{-\infty}^{\infty} s(t)s^*(t-\tau)e^{-j2\pi\upsilon t}dt \tag{1}$$

where τ and υ are the delay and the doppler shift respectively. A perfect radar waveform would have the ambiguity function of the form

$$\chi(\tau, \upsilon) = \delta(\tau)\delta(\upsilon) \tag{2}$$

Michael D. Zoltowski is with the School of Electrical and Computer Engineering, Purdue University, 465 Northwestern Avenue, West Lafayette, IN 47907 mikedz@ecn.purdue.edu

Tariq R. Qureshi is with the School of Electrical and Computer Engineering, Purdue University, 465 Northwestern Avenue, West Lafayette, IN 47907 tqureshi@purdue.edu

Robert Calderbank is with the Center for Applied and Computational Mathematics, Princeton University, Engineering Quadrangle, Olden Street, Princeton, NJ 08544 calderbk@princeton.edu

William Moran is with the Department of Electrical and Electronic Engineering, University of Melbourne, Australia wmoran@unimelb.edu.au

which means that the spike in the ambiguity function would correspond to the correct delay and doppler properties of the target. Construction of waveforms possessing an ambiguity function of this form is a difficult problem in applied mathematics. However, it is not always necessary for the transmitted waveforms to have a thumbtack shaped ambiguity function, particularly if there is only one target or if there are multiple targets that are reasonably well separated in the delay-doppler domain.

In [2], Howard et al. proposed a new multi-channel radar scheme employing polarization diversity for getting multiple independent views of the target. This work is based on processing the transmitted waveform matrix at the receiver in a manner that allows us to separate the transmitted waveforms at the receiver and exploit the diversity inherent in an active sensing environment due to its multipath nature. The waveform separation was achieved through the use of Golay complementary sequences [3]. In this paper, multiple radar waveforms are simultaneously transmitted from different "virtual antenna" elements where each antenna element is a transceiver. The goal is to achieve a thumbtack shaped ambiguity function in the delay domain. The use of the term "virtual antenna" here can also include simultaneous beams formed from the same aperture but pointed to different angles, or beams pointed to the same angle but formed from different sub-apertures. We present an example of a 4×4 system with two dually polarized transceivers. A $4{\times}4$ unitary design dictates the scheduling of the waveforms over the four virtual antennas over four PRIs (Pulse Repetition Intervals) and it tells us how the matched filtering of the returns over four PRIs are combined in such a way so as to achieve both perfect separation (of the superimposed returns) and perfect reconstruction. Perfect reconstruction implies that the sum of the time-autocorrelations associated with each of the four waveforms is a delta function. Conditions for both perfect separation and perfect reconstruction in the delay domain are developed, and a variety of waveform sets satisfying both are presented. Biorthogonal methods are then introduced that can achieve both perfect reconstruction and perfect separation with adaptive waveforms that are matched to the propagation environment.

II. Polarization Diversity Code Design

For a 2×2 system, it has been shown in [2] that for a dually polarized antenna, the OSTBC (Orthogonal Space-Time Block Coded) [4] Golay complementary waveform matrix

$$\mathbf{S} = \begin{bmatrix} e_1[n] & -e_2^*[-n] \\ e_2[n] & e_1^*[-n] \end{bmatrix} \tag{3}$$

978-1-4244-2941-7/08/$25.00 ©2008 IEEE

achieves perfect separation at the receiver. We can extend this idea to the 4×4 case which comprises two dually polarized antennas. We use one Golay pair and the time reversed version of this pair to make four waveforms. The transmitted waveform matrix is given by

$$\tilde{\mathbf{S}}_1 = \begin{bmatrix} \mathbf{S} & -\mathbf{S}^* \\ \mathbf{S} & \mathbf{S}^* \end{bmatrix} \tag{4}$$

where

$$\mathbf{S}^* = \begin{bmatrix} e_1^*[-n] & e_2^*[-n] \\ -e_2[n] & e_1[n] \end{bmatrix} \tag{5}$$

The perfect separation is achieved by observing that

$$\tilde{\mathbf{S}}_1 * \tilde{\mathbf{S}}_1^* = \begin{bmatrix} \mathbf{S}*\mathbf{S}^* + \mathbf{S}^* * \mathbf{S} & \mathbf{S}*\mathbf{S}^* - \mathbf{S}^* * \mathbf{S} \\ \mathbf{S}*\mathbf{S}^* - \mathbf{S}^* * \mathbf{S} & \mathbf{S}*\mathbf{S}^* + \mathbf{S}^* * \mathbf{S} \end{bmatrix} = 2\alpha \mathbf{I}_{2\times 2} \tag{6}$$

These transmitted waveforms are coupled to the receiver through a channel matrix given by

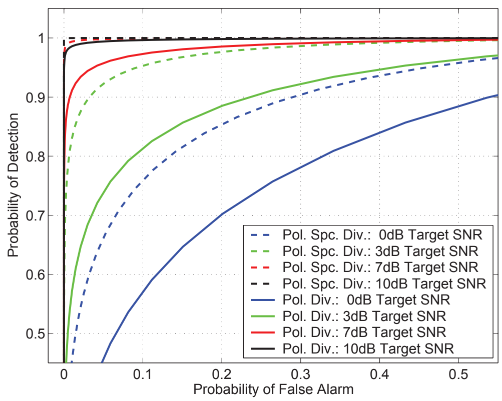

Fig. 1. ROC Curves for baseline, 2x2 and 4×4 systems

$$\mathbf{H} = \begin{bmatrix} h_{11} & h_{12} & h_{13} & h_{14} \\ h_{21} & h_{22} & h_{23} & h_{24} \\ h_{31} & h_{32} & h_{33} & h_{34} \\ h_{41} & h_{42} & h_{43} & h_{44} \end{bmatrix} \tag{7}$$

where h_{ij} is the channel coefficient from the i^{th} transmit antenna to the j^{th} receive antenna. Since the waveforms are perfectly separated at the receiver, we can employ energy detection to detect the presence of the target. In order to perform target detection, we stack the columns of the 4×4 channel coefficient matrix into a vector $\mathbf{T}$ which is given under different hypotheses [5] as:

$$\mathbf{T} = \begin{cases} E_t \mathbf{h} + \mathbf{n} & : H_1 \\ \mathbf{n} & : H_0 \end{cases} \tag{8}$$

where $\mathbf{h}$ is a 16×1 vector of the i.i.d channel coefficients each with variance σ^2, E_t is the energy of the transmitted waveform and $\mathbf{n}$ is the white noise with variance N_0. The likelihood ratio detector is an energy detector that computes the energy in the received vector under both hypothesis and is given by

$$\|\mathbf{T}\|^2 > \gamma \tag{9}$$

where γ is the detection threshold. The probability of false alarm P_F and probability of detection P_D for this case are given by

$$P_F(\gamma) = \sum_{k=0}^{15} \left(\frac{\gamma}{2N_0}\right)^k \frac{e^{\frac{-\gamma}{2N_0}}}{k!} \tag{10}$$

$$P_D(\gamma) = \sum_{k=0}^{15} \left(\frac{\gamma}{2(E_t\sigma^2 + N_0)}\right)^k \frac{e^{\frac{-\gamma}{2(E_t\sigma^2+N_0)}}}{k!} \tag{11}$$

A comparison of the receiver operating curves (ROC) for the 4×4 (Polarization-Spatial Diversity), 2x2 (Polarization Diversity) and baseline systems is given in Figure 1.

III. Conditions for Perfect Separation

Consider a set of waveforms satisfying

$$e_1[n]*e_1^*[-n] + e_2[n]*e_2^*[-n] + e_3[n]*e_3^*[-n] + e_4[n]*e_4^*[-n] \propto \delta[n] \tag{12}$$

We schedule these waveforms over space-time as given by the following matrix, where the rows represent spatial dimensions and columns represent temporal dimensions.

$$\mathbf{E} = \begin{bmatrix} e_1[n] & e_2^*[-n] & e_3[n] & e_4^*[-n] \\ -e_2[n] & e_1^*[-n] & -e_4[n] & e_3^*[-n] \\ -e_3[n] & e_4^*[-n] & e_1[n] & -e_2^*[-n] \\ -e_4[n] & -e_3^*[-n] & e_2[n] & e_1^*[-n] \end{bmatrix} \tag{13}$$

We assume that the channel does not change for the duration of the waveforms that constitute the matrix $\mathbf{E}$. The received waveform matrix $\mathbf{R}$ is given by

$$\mathbf{R} = \mathbf{E} * \delta[n-D] * \mathbf{H} \tag{14}$$

where D is the propagation delay and * denotes convolution. Let us define $\mathbf{E}^*$ as

$$\mathbf{E}^* = \begin{bmatrix} e_1^*[-n] & -e_2^*[-n] & -e_3^*[-n] & -e_4^*[-n] \\ e_2[n] & e_1[n] & e_4[n] & -e_3[n] \\ e_3^*[-n] & -e_4^*[-n] & e_1^*[-n] & -e_2^*[-n] \\ e_4[n] & e_3[n] & -e_2[n] & e_1[n] \end{bmatrix} \tag{15}$$

We process the received waveform matrix $\mathbf{R}$ by $\mathbf{E}^*$, i.e.

$$\mathbf{\Phi} = \mathbf{R} * \mathbf{E}^* \tag{16}$$

and we want

$$\mathbf{\Phi} = \alpha \mathbf{I} \tag{17}$$

where α is a constant. Since the waveforms satisfy (12), we have

$$\mathbf{\Phi}[n-D] = \begin{bmatrix} \delta[n-D] & 0 & -\phi[n-D] & 0 \\ 0 & \delta[n-D] & 0 & \phi[n-D] \\ \phi[n-D] & 0 & \delta[n-D] & 0 \\ 0 & -\phi[n-D] & 0 & \delta[n-D] \end{bmatrix} \tag{18}$$

where

$$\phi[n] = -e_3[n]*e_1^*[-n] + e_4^*[-n]*e_2[n] + e_1[n]*e_3^*[-n] - e_2^*[-n]*e_4^*[-n] \tag{19}$$

We refer to $\mathbf{\Phi}[n]$ as the key matrix. Now, we can see that $\phi[n]$ is conjugate symmetric. i.e.

$$\phi[-n] = -\phi^*[n] \tag{20}$$

which implies that if $\phi[n]$ is real valued, then

$$\phi[0] = 0 \tag{21}$$

We can write $\phi[n]$ as

$$\begin{aligned}\phi[n] = &(-e_3[n] * e_1^*[-n] + e_1[n] * e_3^*[-n]) \\ &+ (e_4^*[-n] * e_2[n] - e_2^*[-n] * e_4^*[-n])\end{aligned} \tag{22}$$

From this, we can see that if all waveforms exhibit conjugate symmetry. i.e.

$$e_i[n] = e_i^*[-n] \quad for \quad i = 1, 2, 3, 4 \tag{23}$$

then

$$\phi[n] = 0 \tag{24}$$

and we achieve perfect separation. Now, consider waveforms that are time-reversed versions of each other, i.e.

$$e_i[n] = e_{i+1}^*[-n] \quad for \quad i = 1, 3 \tag{25}$$

In this case, we also have

$$\phi[n] = 0 \tag{26}$$

Therefore, if the waveforms meet the conditions described above in addition to their respective autocorrelation functions summing to a delta function, we would achieve perfect separation at the receiver.

IV. Waveform families based on Kronecker products

In this section, we explore waveform familes that possess some of the properties outlined in the previous section. The waveform design is based on the Kronecker products [6] of appropriately chosen sequences.

A. Golay Complementary Sequences

Consider two pairs of complementary Golay sequences

$$\varepsilon_1[n] * \varepsilon_1^*[-n] + \varepsilon_2[n] * \varepsilon_2^*[-n] = N_1\delta[n] \tag{27}$$

$$\varepsilon_3[n] * \varepsilon_3^*[-n] + \varepsilon_4[n] * \varepsilon_4^*[-n] = N_2\delta[n] \tag{28}$$

We form the transmitted waveforms of these sequences using the Kronecker product as

$$e_1[n] = \varepsilon_1[n] \otimes \varepsilon_3[n] \tag{29}$$

$$e_2[n] = \varepsilon_1[n] \otimes \varepsilon_4[n] \tag{30}$$

$$e_3[n] = \varepsilon_2[n] \otimes \varepsilon_3[n] \tag{31}$$

$$e_4[n] = \varepsilon_2[n] \otimes \varepsilon_4[n] \tag{32}$$

Consider forming the autocorrelation

$$r[m] = r_{e_1e_1}[m] + r_{e_2e_2}[m] + r_{e_3e_3}[m] + r_{e_4e_4}[m] \tag{33}$$

Since

$$z[n] = x[n] \otimes y[n] \quad \Rightarrow \quad r_{zz}[m] = r_{xx}[m] \otimes_N r_{yy}[m] \tag{34}$$

We have that

$$\begin{aligned}r[m] = &r_{\varepsilon_1\varepsilon_1}[m] \otimes_N r_{\varepsilon_3\varepsilon_3}[m] + r_{\varepsilon_1\varepsilon_1}[m] \otimes_N r_{\varepsilon_4\varepsilon_4}[m] \\ &+ r_{\varepsilon_2\varepsilon_2}[m] \otimes_N r_{\varepsilon_3\varepsilon_3}[m] + r_{\varepsilon_2\varepsilon_2}[m] \otimes_N r_{\varepsilon_4\varepsilon_4}[m] \\ &= N_1N_2\delta[m]\end{aligned} \tag{35}$$

where $\otimes_N$ is the modulo N Kronecker product. From this, we see that the Kronecker product preserves the autocorrelation properties of the original sequences in this case. However, these waveforms don't satisfy the conditions listed in section 3. Let us look at the main and off diagonal sequences of the key matrix of these waveforms by considering two real valued Golay pairs of length 8 and 10 respectively. The main diagonal sequence in the key matrix is shown in Figure 2(a) and the off diagonal sequence $\phi[n]$ as given in the key matrix is shown in Figure 2(b). From these figures, we see that while the main diagonal term is non-zero only at the correct lag value, we do have residual cross-terms in the off diagonal sequence. We also observe that the off diagonal sequence is anti-symmetric, which means that it does not affect the correlation peak at the true lag value, even though $\phi[n]$ is not identically zero in this case.

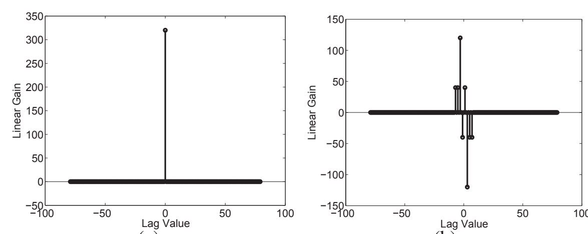

(a) (b)

Fig. 2. (a) Main diagonal sequence: delta function (b) Off diagonal sequence: non-zero values are present

B. Barker Codes

Consider two Barker Sequences

$$b_1[n] = \{1, 1, 1, 1, 1, -1, -1, 1, 1, -1, 1, -1, 1\} \tag{36}$$

$$b_2[n] = \{0, 1, 1, 1, -1, -1, -1, 1, -1, -1, 1, -1, 0\} \tag{37}$$

We form the transmitted waveforms as

$$\begin{aligned}e_1[n] &= b_1[n] \otimes b_2[n] \\ e_2[n] &= e_1^*[-n] \\ e_3[n] &= b_2[n] \otimes b_1[n] \\ e_4[n] &= e_3^*[-n]\end{aligned} \tag{38}$$

These waveforms satisfy one of the conditions for perfect separation given in section II but their autocorrelation functions don't sum to a perfect delta function. The diagonal and off-diagonal autocorrelation sequences are given in Figure 3(a) and 3(b). Unlike the Golay complementary codes, these sequences are not identically zero except at the true lag position in the main diagonal. However, the off diagonal

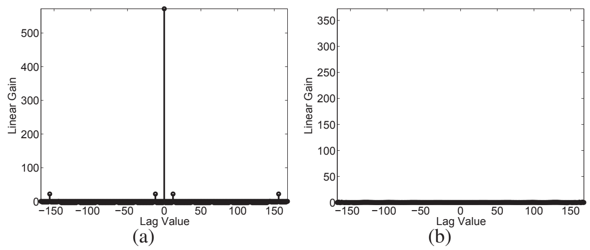

Fig. 3. (a) Main diagonal sequence: some of values around the main lobe are non-zero (b)Off diagonal sequence is identically zero

terms are identically zero because of the fact that these waveforms are time-reversed versions of each other.

C. Conjugate Symmetric Transmit Waveforms

In this section, we look at waveforms that exhibit conjugate symmetry. An important aspect in the design of conjugate symmetric waveforms is their DFT (Discrete Fourier Transform) properties. Since the DFT of a conjugate-symmetric sequence is real valued, the use of conjugate-symmetric sequences enables 2x2, 4×4 and 8x8 waveform scheduling according to OSTBC for real designs [4]. Figure 4(a) shows the SRRC (Square Root Raised Cosine) quarter-band filter impulse response given by

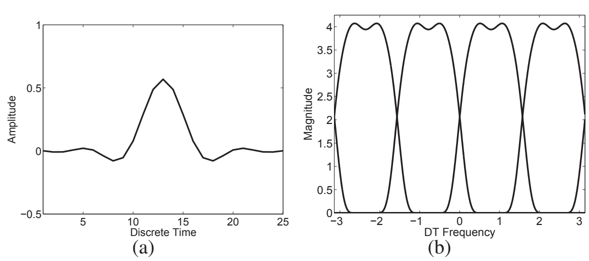

Fig. 4. (a) Impulse response of the quarter-band filter (b) Frequency response of the four quarter-band filter waveforms

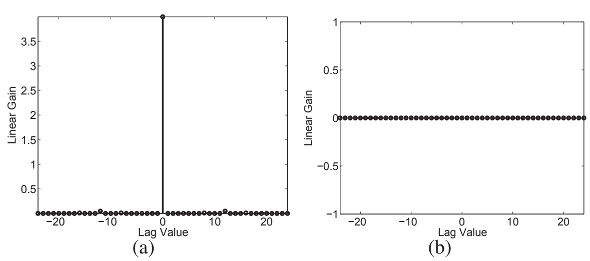

Fig. 5. (a) Main diagonal sequence is close to a delta function (b) Off diagonal sequence is identically zero

$$h(t) = \frac{\frac{4\alpha t}{T}\cos\left(\frac{(1+\alpha)\pi t}{T}\right) + \sin\left(\frac{(1-\alpha)\pi t}{T}\right)}{\frac{\pi t}{T}\left[1-\left(\frac{4\alpha t}{T}\right)^2\right]} \tag{39}$$

In order to make four conjugate symmetric waveforms using the pulse waveform given by (39), we sample the pulse with a sampling interval $T_s = \frac{T}{4}$. The combined frequency response of these waveforms is shown in Figure 4(b). The main and off diagonal sequences of the key matrix for these waveforms are given in Figure 5(a) and 5(b). We see from these figures that these waveforms are almost perfectly separable, with some minor disturbances in the main diagonal due to the time limiting of the SRRC waveforms.

D. Combination of Golay Codes and Half Band Filters

In the previous section, we created waveforms with quarter-band filters that achieved perfect separation. In this section, we form transmit waveforms through the Kronecker product of Golay codes with half-band SRRC filters. The transmit waveforms are given by

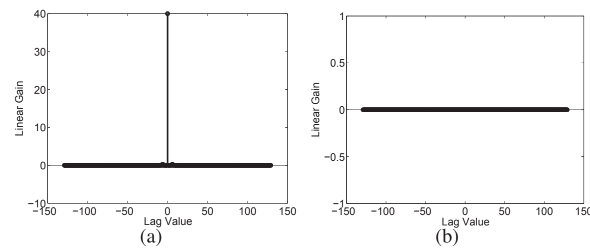

Fig. 6. (a) Main diagonal sequence resembles a delta function (b) Off diagonal sequence is identically zero

$$\begin{aligned} e_1[n] &= g_1[n] \otimes h_1[n] \\ e_2[n] &= g_1[n] \otimes h_2[n] \\ e_3[n] &= g_2[n] \otimes h_1[n] \\ e_4[n] &= g_2[n] \otimes h_2[n] \end{aligned} \tag{40}$$

where $g_i[n]$ are the Golay codes and $h_i[n]$ are the half-band filters. The main and off diagonal sequences of the key matrix are shown in Figures 6(a) and 6(b) . We see that the Kronecker product formed from the combination of Golay sequences with half-band filters possess excellent separation properties.

V. DATA DEPENDENT WAVEFORM DESIGN

So far, we have discussed waveform design without considering the effects of clutter and interference. In a physical active sensing environment, we desire to transmit waveforms that depend on the clutter and interference environment, e.g., waveforms that are orthogonal to the clutter subspace. Let the transmitted waveform and the receiver processing matrices be given by

$$\mathbf{E}_T = \begin{bmatrix} e_1[n] & f_2^*[-n] & e_3[n] & f_4^*[-n] \\ -e_2[n] & f_1^*[-n] & -e_4[n] & f_3^*[-n] \\ -e_3[n] & f_4^*[-n] & e_1[n] & -f_2^*[-n] \\ = e_4[n] & -f_3^*[-n] & e_2[n] & f_1^*[-n] \end{bmatrix} \tag{41}$$

$$\mathbf{E}_R = \begin{bmatrix} f_1^*[-n] & -f_2^*[-n] & -f_3^*[-n] & -f_4^*[-n] \\ e_2[n] & e_1[n] & e_4[n] & -e_3[n] \\ f_3^*[-n] & -f_4^*[-n] & f_1^*[-n] & f_2^*[-n] \\ = e_4[n] & e_3[n] & -e_2[n] & e_1[n] \end{bmatrix} \tag{42}$$

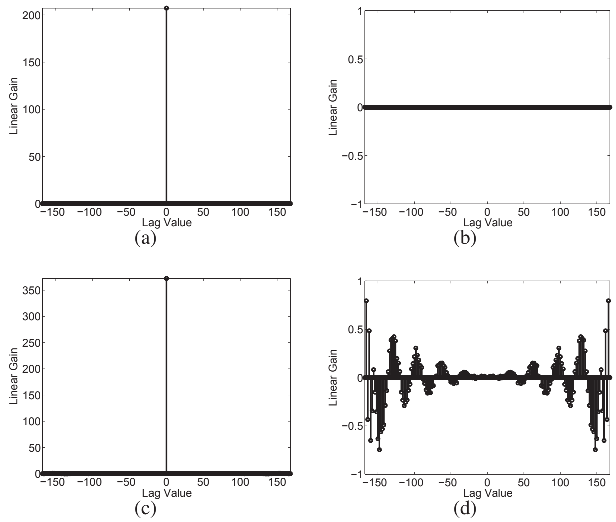

Fig. 7. (a) Discarding more singular values reduces the peak but removes the unwanted non-zero values (b) Off diagonal sequence is zero if we discard more singular values (c) Discarding fewer singular results in a higher peak compared to (a) and removes the unwanted non-zero values (d) Off diagonal sequence is not identically zero if we discard fewer singular values

The general problem can now be expressed as

$$\mathbf{E}_T * \delta[n-D] * \mathbf{E}_R \propto \delta[n-D]\mathbf{I} \tag{43}$$

In order for the waveforms to satisfy (43), the following conditions should be satisfied

$$\begin{aligned} \phi[n] = -e_3[n] * f_1^*[-n] + f_4^*[-n] * e_2[n] \\ +e_1[n] * f_3^*[-n] - f_2^*[-n] * e_4[n] = 0 \end{aligned} \tag{44}$$

$$\begin{aligned} r[n] = e_1[n] * f_1^*[-n] + e_2[n] * f_2^*[-n] \\ +e_3[n] * f_3^*[-n] + e_4[n] * f_4^*[-n] \propto \delta[n] \end{aligned} \tag{45}$$

We can express both these constraints in the form of a matrix equation as

$$\mathbf{E}'\mathbf{F} = \begin{bmatrix} \mathbf{E}_1 & \mathbf{E}_2 & \mathbf{E}_3 & \mathbf{E}_4 \\ -\mathbf{E}_3 & -\mathbf{E}_4 & \mathbf{E}_1 & \mathbf{E}_2 \end{bmatrix} \begin{bmatrix} \mathbf{f}_1 \\ \mathbf{f}_2 \\ \mathbf{f}_3 \\ \mathbf{f}_4 \end{bmatrix} = \begin{bmatrix} \delta[n-D] \\ \mathbf{0} \end{bmatrix} \tag{46}$$

where $\mathbf{E}'$ is a $2(2N-1) \times 4N$ convolution matrix where the rows represent the delayed and flipped waveform sequences. This means that we have $2(2N-1)$ equations in $4N$ unknowns and since there are more unknowns than the number of equations, this system is under-determined and there are multiple solutions. The best solution for our problem is the one that maximizes

$$\begin{bmatrix} \mathbf{e}_1^T & \mathbf{e}_2^T & \mathbf{e}_3^T & \mathbf{e}_4^T \end{bmatrix} \begin{bmatrix} \mathbf{f}_1 \\ \mathbf{f}_2 \\ \mathbf{f}_3 \\ \mathbf{f}_4 \end{bmatrix} \tag{47}$$

We saw in the case of the Kronecker products of Barker codes that the main diagonal term had non-zero values around the main lobe, even though they were very small. We apply this analysis to the Kronecker products of Barker codes. We do an SVD (Singular Value Decomposition) on the matrix $\mathbf{E}'$ constructed from Barker codes and apply a threshold to the singular values. This lets us affect a trade-off between the non-zero terms on the main diagonal and off diagonal and the peak of the main diagonal at the true target delay. Figure 7 shows the results for two-different thresholds. We can see from here that if we discard a small number of singular values, there is a peak loss of about 1.8dB (Fig 7(c)) and the off-diagonal terms are slightly higher (Fig(7(d)), but there are no other non-zero terms in the main diagonal. If we discard more singular values, the peak loss increases to about 4.1 dB (Fig 7(a)) but there are no unwanted non-zero terms in either the main diagonal or the off diagonal (Fig 7(b)). This shows the amount of flexibility we have with the waveform design when we pose this problem in a more general setting.

VI. Conclusions and Future Work

In this paper, we explored the problem of perfect waveform separation at the receiver in an active sensing environment for the 4×4 case. We derived conditions that the four waveforms need to satisfy in order to achieve perfect separation at the receiver. We explored waveform families that achieve perfect reconstruction at the receiving end. We showed that Golay codes, Barker codes and quarter-band filters possess good separation properties and if we construct waveforms using a combination of these constituent waveforms through the use of Kronecker products, we can achieve very good separation at the receiver. We also addressed the problem of data dependent waveform design in which the transmitted waveforms are dependent on the clutter and interference present in the active sensing environment. We showed that by controlling the number of singular values of the waveform matrix, we can reduce interference at the expense of detection performance.

In the future, we would explore the Doppler properties of the waveform families described in this paper. We also intend to explore the problem of designing data dependent waveforms in more detail, both from the delay and the Doppler perspective, as well as incorporate beamforming at the transmitting and the receiving ends to be able direct the illuminating beams in specific directions.

References

[1] N. Levanon, *Radar Principles*, Wiley-interscience, 2001.

[2] S.D. Howard, A.R. Calderbank, and W. Moran, "A Simple Polarization Dversity Scheme for Radar Detection", in *Proc. of Second Intl. Conf. on Waveform Diversity and Design*, 22-27, (2006).

[3] M.J.E. Golay, "Static Multislit Spectrometry and Its Applications to the Panoramic Display of Infrared Spectra," *J. Optical Soc. Amer.*, 41, 468-472, (1951).

[4] V. Tarokh, H. Jafarkhani, and A.R. Calderbank, "Space-Time Block Codes from Orthogonal Designs", *IEEE Trans. on Information Theory*, 45, 1456-1467, (1999).

[5] S.M. Kay, *Fundamentals of Statistical Signal Processing, Vol. 2: Detection Theory*, Prentice Hall, 1993.

[6] A.H. Roger, and C.R. Johnson, *Topics in Matrix Analysis*, Cambridge University Press, 1991.